Solvation of Radical Cations in Water—Reactive or Unreactive Solvation?

Matthias Mohr,[a] Dominik Marx,[b] Michele Parrinello,[c] and Hendrik Zipse*[a]

Abstract: The solvation and reaction of ethylene radical cation in aqueous solution has been studied with Car–Parrinello molecular dynamics simulations. All ab initio simulations were performed using a system of 56 water and one ethylene molecule. Using a favorable symmetrically solvated radical cation as the starting point of the simulation a fast addition of water (within 90 fs) to the radical cation is observed. The primary addition product is rapidly deprotonated (within 100 fs) to yield the ethanol-2-yl radical. A second simulation was initiated through vertical ionization of neutral hydrated ethylene, representing a significantly less favorable situation for the addition process. No addition of water can be observed in this second simulation over a time span of 1.7 ps. Taken together the two simulations are indicative of a rearrangement of the solvent shell which represents the major part of the overall reaction barrier. Under these circumstances, the reaction rate of an otherwise spontaneous reaction is limited by the intrinsic solvent relaxation time. This interpretation of the reactivity of hydrated radical cations reconciles previously conflicting experimental condensed phase and theoretical gas phase studies.

Keywords: density functional calculations · molecular dynamics · radical ions · solvent effects · water

Introduction

How do radical cations interact with the surrounding solvent? This question is essential to the solution chemistry of radical cations including systems of biological[1] as well as synthetic[2] relevance. We have recently studied the interaction of water molecules with simple alkene radical cations such as those of ethylene (**1**) and *trans*-2-butene at several different levels of theory.[3, 4] For these small radical cations, two limiting cases[4] can be envisioned for solute–solvent interactions: "unreactive solvation" without covalent bond formation (as in **2**) and "reactive solvation" with covalent bond formation between solute and solvent (as in **3**).

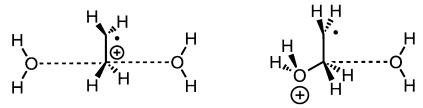

2 **3**

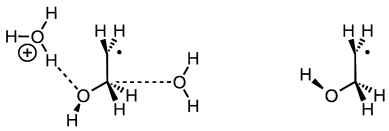

4 **5**

All theoretical studies of the interaction of water with small alkene radical cations[3, 4] predict barrier-free reaction between solvent and solute and thus favor reactive solvation as the most realistic scenario. The same result has been obtained in theoretical studies of the reaction of small alkene radical cations with acetonitrile,[5] one of the most commonly used solvents in preparative radical cation chemistry. These results are at variance with the experimental observation that radical cations react with alkenes much faster than with typical solvents such as acetonitrile or methanol.[6, 7] This experimental finding is also in line with the fact that the synthetically used radical cation mediated [2 + 2] cycloaddition of alkenes proceeds without incorporation of nucleophilic solvent molecules in most cases.[8–10] The qualitative discrepancy between computational results and experimental observation might be

[a] Prof. Dr. H. Zipse, Dr. M. Mohr
Department Chemie, Ludwig-Maximilians-Universität München
Butenandt-Strasse 5–13, 81377 München (Germany)
Fax: (+49) 89-2180-7734
E-mail: zipse@cup.uni-muenchen.de

[b] Prof. Dr. D. Marx
Lehrstuhl für Theoretische Chemie
Ruhr-Universität Bochum, 44780 Bochum (Germany)
Fax: (+49) 234-32-14045
E-mail: dominik.marx@theochem.ruhr-uni-bochum.de

[c] Prof. Dr. M. Parrinello
Max-Planck-Institut für Festkörperforschung
Postfach 800 665, 70506 Stuttgart (Germany)
Fax: (+49) 711-689-1702
E-mail: prr@prr.mpi-stuttgart.mpg.de

Supporting information for this article is available on the WWW under http://www.wiley-vch.de/home/chemistry/ or from the author.

  0947-6539/00/0621-4009 $ 17.50+.50/0

due to the neglect of bulk solvation effects in previous theoretical studies. It is clear from earlier studies that solvent effects will have a significant influence on the energetic difference between **2** and **3**.[3] More importantly additional solvent molecules will be actively involved in reaction steps leading from **3** to other reactive intermediates such as complex **4**, the ethanol-2-yl radical (**5**) in various states of solvation, and ultimately to closed shell reaction products. In order to clarify this point we have now performed solution simulations of ethylene radical cation (**1**) in aqueous solution. As radical cation **1** appears to be highly reactive towards single water molecules, a realistic description of **1** in bulk water necessitates a quantum mechanical description of the electronic structure of both solvent and solute. The method of choice for such a case is the Car–Parrinello method,[11, 32] which is known to provide a very good description of liquid water[12] as well as solvation effects of cations in water[13] and of chemical reactions.[11, 32] The results obtained in such a simulation will, of course, depend considerably on the initial conditions. We have therefore chosen two very different starting configurations for our simulations. The first simulation **A** was initiated from symmetric structure **2**, which according to gas phase calculations at the UMP2/6–31G(d) level of theory[3] is a transition state for water exchange. An earlier study using a combination of ab initio electronic structure calculations and empirical Monte Carlo solution simulations found that **3** was better solvated than **2** by 5–8 kcal mol^{-1}.[3] The structure of **2** is reminiscent of the solvation of symmetric carbocationic intermediates in polar solution.[15] If symmetric solvation (as in **2**) is less favorable than reactive solvation (as in **3**) even in solution a rapid addition of one of the water molecules in **2** to the hydrocarbon substrate would be expected. A second simulation **B** has been initiated from neutral ethylene equilibrated in water and then vertically (that is, without prior relaxation of structural parameters) ionized during the course of the simulation. The initial solvent structure around the alkene radical cation is therefore that of neutral ethylene. In contrast to simulation **A** the water addition process will likely be more difficult under these conditions as substantial relaxation of the first solvation shell will be required before a successful addition event.

Computational methods

All simulations were performed under periodic boundary conditions. "Pre-equilibration" of the systems was achieved through Monte Carlo (MC) simulations using classical potentials.[16] The TIP4P model was used for water. Standard all-atom Lennard–Jones parameters were used for ethylene[16] while the parameters for **2** were those developed in our earlier study.[3] MC simulations were performed at 25 °C and 1 atm in the NPT ensemble (constant number of particles, constant pressure, constant temperature). The structure of the solutes (**2** or ethylene) was held rigid during the equilibration runs. Cutoff distances for electrostatic interactions were set to 6.0 Å for substrate–solvent as well as solvent–solvent interactions. Simulations were continued until a permanent change in volume was no longer observed and the solute–solvent radial distribution functions (rdf) had converged to a constant picture.

All Car–Parrinello molecular dynamics (CPMD) simulations were performed with the CPMD program[17] using a spin polarized semilocal BLYP functional[18] and a cubic box under periodic boundary conditions. The wavefunction was expanded at the Γ-point in a plane wave basis set with a kinetic energy cutoff of 70 Ry, while the 1s electrons of the non-hydrogen atoms were represented by norm-conserving pseudopotentials of the Troullier–Martins type.[19] The timestep for the numerical integration of the equations of motion according to the velocity Verlet algorithm was set to 0.12 fs. The treatment of the nuclei was purely classical and can therefore not account for quantum mechanical effects. Simulations on positively charged species were performed with the corresponding negative charge distributed uniformly in the cubic cell.[20]

Results

Simulation A: Starting from structure 2

The starting point for simulation **A** was obtained by surrounding rigid structure **2** randomly with 54 water molecules in a cubic box. This system was then equilibrated using repeated batches of 3×10^6 MC steps until both the rdfs for the substrate and the volume of the system had converged to constant values. As it was not clear at the outset of this study whether simulations in such a small solvent box would give meaningful results in terms of solvent structure, a larger cubic box containing **2** and 263 TIP4P water molecules was treated in the same way. The H(substrate **2**)–O(TIP4P) radial distribution function g_{OH} is most descriptive of the solvation shell around substrate **2** and is depicted for both systems in Figure 1. It can readily be seen that the first and also the

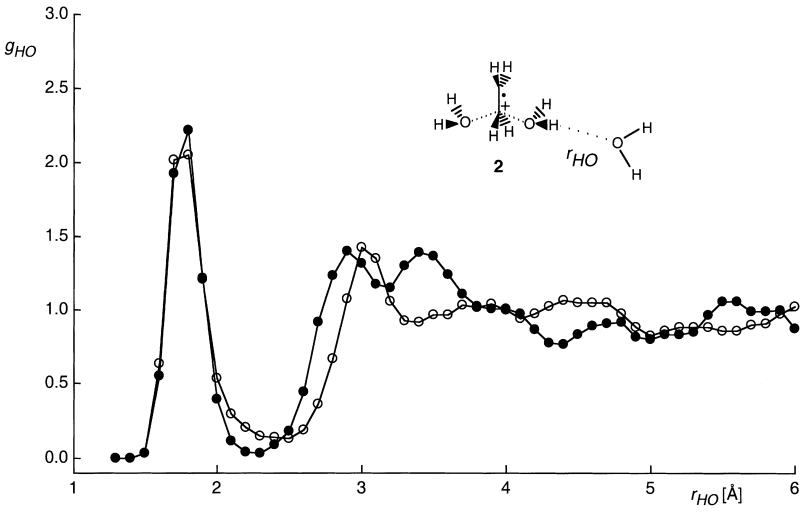

Figure 1. Radical distribution function g_{HO} for the H(substrate **2**)–O(water) distance in a cubic box of 54 (filled circles) or 263 (empty circles) TIP4P water molecules obtained after MC equilibration.

0947-6539/00/0621-4010 $ 17.50+.50/0 *Chem. Eur. J.* **2000**, *6*, No. 21

second solvation shell up to 3 Å away from the water moieties contained in **2** are described in a similar manner in both systems. It is only beyond a distance of 3 Å that small deviations occur. The solvation shell is dominated by one prominent peak at 1.8 Å reflecting the strong hydrogen bonds formed by the water molecules held rigid in **2** to the closest solvating water molecules. The system finally chosen as the starting point for the CPMD run had an edge length of 11.2 Å. Neglecting the ethylene moiety, this corresponds to a water density of 1.19 g cm^{-3}.

Upon initiation of the CPMD simulation, structure **2** is converted to **3** within 90 fs. The addition process can be monitored by the time evolution of the distance between the ethylene carbon atoms and the closest water molecule (Figure 2). Starting from a value of 2.27 Å (as in **2**) the carbon oxygen bond length reached a minimum value of 1.4 Å after

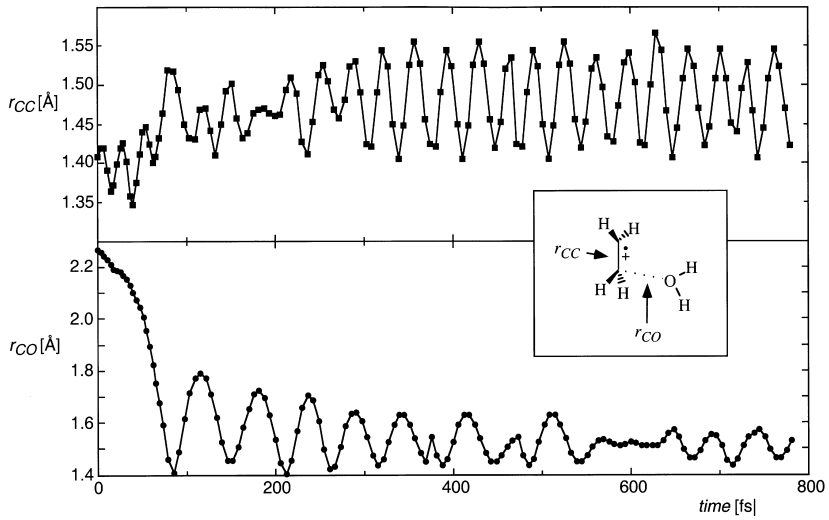

Figure 2. Time evolution of the C–O (filled circles) and C–C (filled squares) distances during simulation **A**.

90 fs. The vibrational amplitude of the newly formed C–O bond becomes even smaller over the following 500 fs and remains constant thereafter. Formation of the new C–O bond is accompanied by elongation of the former ethylene C–C bond. Starting from an initial value of 1.41 Å the addition of water leads to an average value of 1.48 Å within 300 fs (Figure 2).

Unlike in the gas phase, adduct **3** does not represent a stable species in aqueous solution as rapid deprotonation occurs to give structure **4**. The deprotonation process can easily be detected in a plot of the H–O bond distance of adduct **3** as a function of time (Figure 3), which shows a sudden increase after 190 fs, indicating proton transfer from the reacting water molecule to an adjacent solvating water molecule. After this proton transfer step has occurred, the H-O stretching vibrations are overlaid by a large amplitude vibration between the ethanol-2-yl radical (**5**) and the hydronium ion contained in **4**. Complex **4** exists for approximately 450 fs. At this point, a second proton transfer occurs from the former hydronium ion to an adjacent water molecule. The overall sequence of events is summarized in Figure 4.

The lifetime of symmetrically solvated radical cation **2** in aqueous solution is very short and the addition of water is complete within 90 fs. This rapid addition process indicates that charge localized species **3** is better solvated than **2**, in which the positive charge is formally delocalized over two carbon atoms. The lifetime of adduct **3** is also rather limited in aqueous solution due to rapid deprotonation (within 100 fs) and formation of **4**. Complex **4** donates a proton to one of the adjacent water molecules after another 450 fs to yield ethanol radical **5** surrounded by neutral water molecules. While no further reaction can be observed for radical **5** in our simulation, this latter species will have a short lifetime under most experimental conditions.

The rapid addition of one of the water molecules in **2** is only possible if no major rearrangement of the solvent structure is required for this step. This implies that the higher reactivity of one of the equidistant water molecules in **2** over the second one is likely to be a consequence of the solvent structure at the initiation point of the CPMD simulation. This is illustrated in Figure 5a, which shows structure **2** together with the six closest solvating water molecules at the starting point of the CPMD simulation. The two equidistant water molecules **a** and **b** in **2** are both surrounded by three solvating water molecules such that two of these act as hydrogen bond acceptors and the third as a hydrogen bond donor. The hydrogen bond distances are, however, considerably different for **a** and **b**. Both hydrogen bonds donated by **a** are shorter than those donated by **b** (1.65/1.91 Å vs 1.70/1.97 Å) and the same can be observed for hydrogen

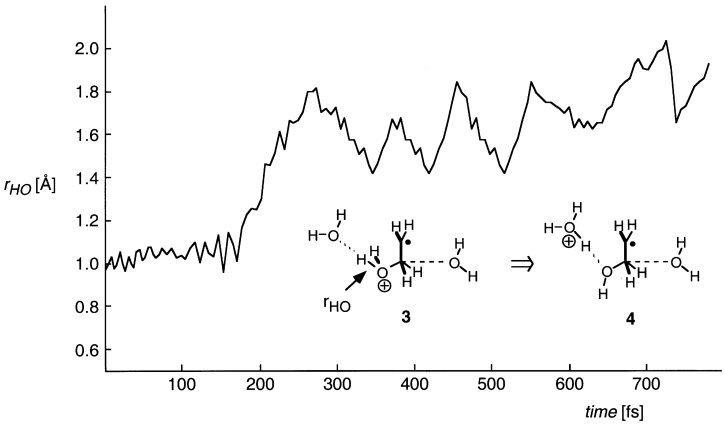

Figure 3. Time evolution of the H–O distance r_{HO} during deprotonation of the previously formed adduct **3** in simulation **A**.

bonds accepted by **a** and **b** (1.79 vs 2.33 Å); the largest distance in **b** is actually beyond the limit of what one might accept for a proper hydrogen bond. The less favorable solvation of **b** is a consequence of the orientation of two of the solvating water molecules which precludes the formation

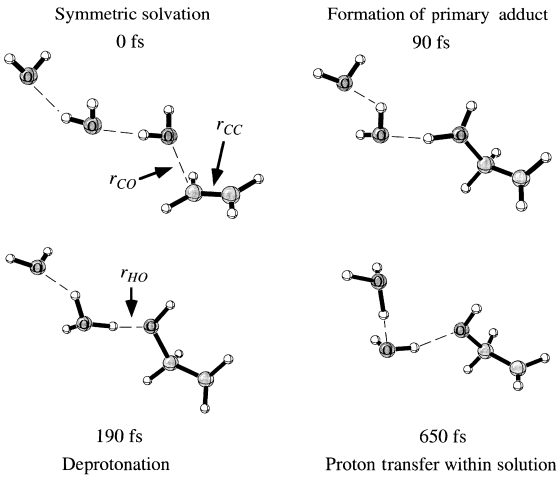

Figure 4. Main stages of reaction of radical cation **2** in aqueous solution. See Figure 2 and Figure 3 for time evolution of distances r_{CO}, r_{CC}, and r_{OH}. Covalent and hydrogen bonds are shown by solid and dashed lines.

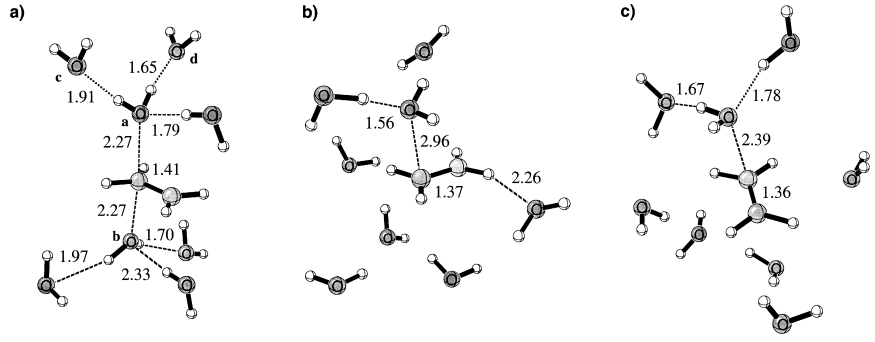

Figure 5. a) Rigid structure **2** together with the six closest solvating water molecules at the starting point of simulation **A**. The two equidistant water molecules contained in **2** are labeled as **a** and **b**. b) Snapshot of ethylene with eight closest water molecules obtained at the end of the CPMD simulation of neutral ethylene with 56 water molecules before the vertical ionization event. c) Snapshot of ethylene with the eight closest water molecules at the point of closest carbon–oxygen distance as observed in simulation **B**. All distances are given in Å.

of strong hydrogen bonds. Formation of stronger hydrogen bonds will polarize water **a** probably in such a way that it becomes the more potent nucleophile and thus more reactive. The solvent structure at the starting point of the CPMD simulation also has a pronounced effect on the proton transfer steps observed after formation of the initial addition product **3**. Of the two water molecules directly hydrogen bonded to water molecule **a** (Figure 5a) it is the more distant water molecule **c** (H–O distance 1.91 Å) that ends up abstracting a proton and not the closer solvating water molecule **d** (H–O distance 1.65 Å)! This counterintuitive reactivity appears to be due to differences in the first solvation shell between the more and the less reactive water molecules: within a cutoff value for the O–O distance of 3.25 Å, the more reactive water molecule **c** is surrounded by overall five other water molecules, while the less reactive one **d** is surrounded by only three water molecules.[21] Thus, the proton is transferred to an "undercoordinated water molecule" in accordance with the findings in ab initio simulations of proton transfer.[13b, 22, 23] Moreover, the first solvation shell **c** is significantly more compact as compared to its less reactive competitor **d**. While the numbers of nearest neighbors change at around 80 fs in the simulation, the compactness of the first solvation sphere of the more reactive water molecule persists until the proton transfer step occurs at 190 fs. We can therefore conclude that both the higher reactivity of water **a** as compared to water **b** as well as the selectivity observed in the subsequent proton transfer steps are a consequence of the solvent structure around the respective water molecules.

Simulation B: Starting from neutral ethylene

The starting point for simulation **B** was obtained by surrounding neutral ethylene with 56 water molecules in a cubic box. Preequilibration of this system was achieved in the same way as in simulation **A** and required three sets of 3×10^6 MC steps. The system finally chosen as the starting point of the CPMD simulation had an edge length of 12.6 Å. This choice leads to a significantly larger volume of the simulation box due to hydrophobic solvation and consequently to a smaller density of water molecules as compared to simulation **A**. Besides the unfavorable structure of the first solvation shell for the addition reaction, this lower density represents a second factor limiting the chances of a successful addition event. A first CPMD run of 100 fs was performed on the neutral system to allow for further relaxation, now using a quantum mechanical description of the electronic subsystem. The MC as well as the CPMD simulations of the neutral system agree in that the solvent structure around neutral ethylene is very different from that of the corresponding radical cation. In addition it is more or less in line with expectations for a hydrophobic hydrocarbon. A typical snapshot from these simulations is shown in Figure 5b, which has been obtained after 100 fs of CPMD simulation and represents, after ionization, the starting point of the cationic part of simulation **B**. There is significant free space above and below the ethylene π system and the closest water oxygen atom is located 2.96 Å away from the ethylene carbon atoms, in significant contrast to a distance of only 2.27 Å in simulation **A**. A somewhat smaller distance of 2.26 Å can be noted between the ethylene hydrogen atoms and the closest water oxygen atom. At the point of ionization the ethylene moiety itself is caught in a maximum of the C–C bond stretching vibration and the C–C bond length of 1.37 Å is thus significantly longer than the distance in isolated ethylene of 1.33 Å (BLYP value obtained by CPMD). As our primary interest here lies in the addition of water to the ethylene framework after ionization, the distance between the closest water oxygen atom and one of the two ethylene carbon atoms has been depicted in Figure 6 together with the time dependence of the ethylene C–C bond distance. It must be emphasized that the distance r_{CO} does not always refer to

  0947-6539/00/0621-4012 $ 17.50+.50/0 *Chem. Eur. J.* **2000**, *6*, No. 21

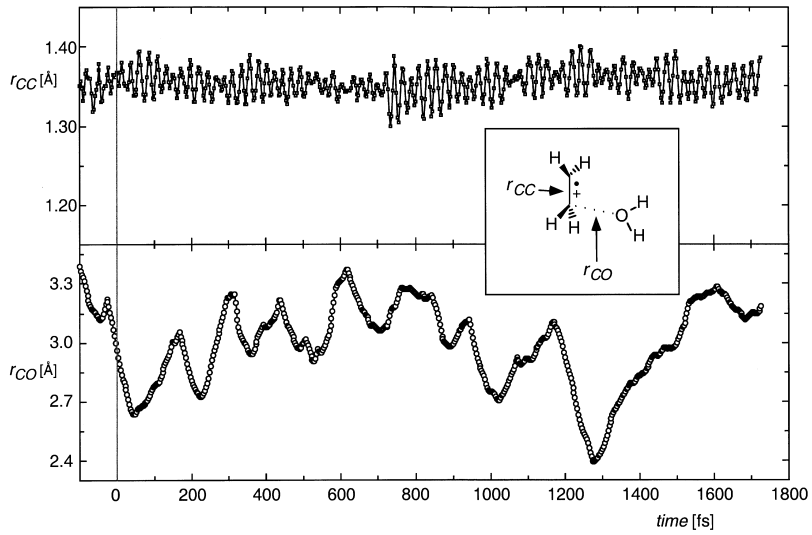

Figure 6. Time evolution of C–O (open circles) and C–C (open squares) distances during simulation **B**. The vertical line at 0 fs marks the ionization event.

the same water molecule, but rather to the water molecule closest to the ethylene carbon atoms at a given time step of the simulation. The zero point in time corresponds to the point of ionization and previous parts of the trajectory correspond to the CPMD simulation performed on the neutral system. In contrast to simulation **A**, no addition of water to ethylene occurs in simulation **B** after ionization within a simulation time of 1.7 ps. Inspection of the variation of the C–O bond distance between the water oxygen and the ethylene carbon atoms in Figure 6 shows that the solvent has never approached the ethylene carbon atoms closer than 2.4 Å, the closest approach occurring after about 1.3 ps. This point is structurally quite similar to the starting point of simulation **A** (at 2.27 Å), but C–O bond formation does not occur in case **B**. A snapshot of this point of simulation **B** is given in Figure 5c. The attacking water molecule appears to be part of a water trimer forming two hydrogen bonds to its nearest neighbors. Even more surprisingly, the length of the ethylene C–C bond appears to be barely influenced by either the ionization process or the approach of solvent molecules (upper panel in Figure 6). During the course of the cationic simulation of run **B**, the C–C bond distance oscillates between 1.30 and 1.40 Å with an average of 1.355 Å. This value is practically identical to that of the preceding neutral simulation (1.352 Å), and the average of the first 750 fs of the cation part of the simulation is practically identical to that of the second half (1.353 Å vs 1.357 Å). These structural data imply that only little of the positive charge and thus of the unpaired spin density is actually located on the ethylene substrate but that most of it must be delocalized over the surrounding solvent.

These results are possibly due to deficits of the semilocal BLYP functional. The artificial stabilization of spin-delocalized states has been noted several times before, especially for radical cations of symmetric species.[24, 25] It has been suggested by Yang[26] that these problems arise through self-interaction errors[27] inherent in pure generalized gradient approximation (GGA) methods and that significant improvements can be realized upon admixture of some fraction of Hartree–Fock exchange. According to the analysis of Yang[26] the amount of self-interaction is largest for systems that contain singly and doubly occupied orbitals of comparable energy. In such a case delocalization of electron spin density will be predicted to be artificially stable. In order to trace our observations back to this effect we calculated the ionization energies of the species shown in Figure 7. Besides ethylene (**1**) and a single water molecule (**6**) we investigated the water dimer **7** and trimer **8**. Structure **9** represents an assembly of four water molecules taken from CPMD simulation **B** at the point of ionization. The central water molecule X of structure **9** corresponds to that water molecule in simulation **B**, which shows the largest amount of spin density in the system. Structure **9** was not optimized on the corresponding level of theory in order to investigate the behavior of water assemblies present in simulation **B**. In all other cases, the systems were first optimized in the neutral state and then vertically ionized to the corresponding radical cations. Table 1 shows a summary of the vertical ionization energies calculated in this manner at the BLYP/6–31+G(d,p) and BHLYP/6–31+G(d,p) levels of theory.[28] The difference between the ionization energies of ethylene (**1**) and water (**6**) on the BLYP/6–31+G(d,p) level of theory of 51.9 kcal mol^{-1} appears to be large enough to prevent the BLYP functional from predicting artificially stable electron densities in the sense of Yang's explanation. Addition of a second water molecule as in water dimer **7**

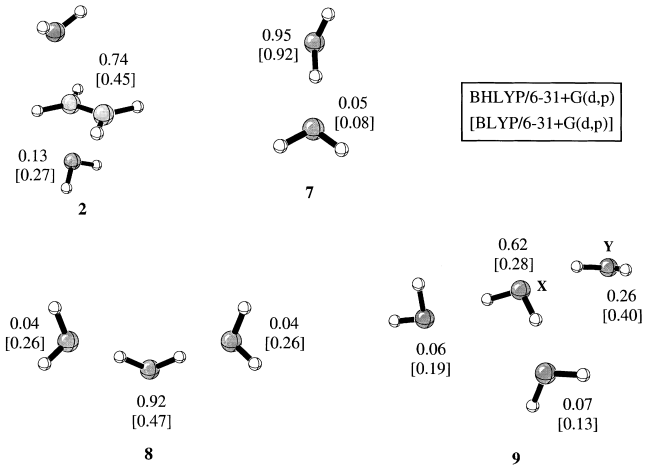

Figure 7. Cumulative Mulliken partial charges of the structures **2**, and **7–9** obtained after vertical ionisation of the neutral species. Upper values have been calculated at the BHLYP/6–31+G(d,p)-level, lower values at the BLYP/6–31+G(d,p)-level of theory. Water molecule **X** of structure **9** represents the water molecule of simulation **B**, at which the largest spin density is located.

Table 1. Summary of the ionization energies of structures **1**, **2**, **6**–**9** calculated at the BHLYP/6–31+G(d,p) and BLYP/6–31+G(d,p) levels of theory. All values are given in kcal mol^{-1}.

	BHLYP/6–31+G(d,p)	BLYP/6–31+G(d,p)	Exptl.[a]
C_2H_4 (**1**)	235.8	240.0	242.2
H_2O (**6**)	286.2	291.9	291.0
$(H_2O)_2$ (**7**)	263.5	268.7	258.5
$(H_2O)_3$ (**8**)	246.7	230.8	–
complex **2**	170.9	168.8	–
$(H_2O)_4$ (**9**)	241.8	211.2	–

[a] Experimental data taken from ref. [29].

reduces the ionization energy by 23.7 kcal mol^{-1} compared to **6**, and addition of a third water molecule leads to another drop of 37.9 kcal mol^{-1}, now 9.2 kcal mol^{-1} below the ionization energy of ethylene! An even lower value can be calculated for water tetramer **9** with an ionization energy of 211.2 kcal mol^{-1}.

How reliable are these theoretical results? Experimental values are available for systems **1**, **6**, and **7**.[29] In all three cases the BLYP predictions are fairly close and the largest deviation occurs for water dimer **7**. In this case the BLYP value is too high by approximately 10 kcal mol^{-1}, certainly not indicative of the problems noted for the larger systems. Inspection of the BHLYP values for these smaller systems also shows that admixture of Hartree–Fock exchange contributions does *not* lead to systematic improvement for these three systems. However, BHLYP predicts the ionization energies for the water clusters **8** and **9** to be higher than for ethylene, while the reverse order is predicted by BLYP. The difference between the ionization energies of ethylene and water tetramer **9** does become quite small, however, even at the BHLYP level of theory. Overall Mulliken charges calculated for the water and ethylene fragments of structures **2** and **7**–**9** (Figure 7) support the notion of artificial stabilization of delocalized states at the BLYP level of theory. In water dimer **7** the difference between BLYP and BHLYP partial charges amounts to 0.03 e, whereas for water trimer **8** a much larger difference can be observed: While the central water molecule in **8** carries a positive partial charge of +0.92 e at the BHLYP level of theory, a much smaller value of +0.47 e is found at the BLYP level. For structure **9** a similar result is observed in that the central water molecule X carries a charge of +0.62 e at the BHLYP level and of +0.28 e with BLYP level. Inspection of the lowest lying electronic states of ionized cluster **8** in C_{2v} geometry reveals that the changes in spin and charge density are due to selective stabilization of delocalized states at the BLYP level of theory. The BHLYP functional predicts the $^2B_1$ state to be more stable than the $^2A_1$ state, while the reverse order is predicted using the BLYP functional.[30]

In summary, we can conclude that differential ionization energies as well as charge and spin density distributions of the semilocal BLYP functional are in line with Yang's explanation of artificial stabilization through electron delocalization. This results in a much lower ionization energy predicted by the BLYP as compared to the hybrid BHLYP functional. Considering this conclusion it is not obvious why simulation **A** worked well. To address this question we calculated the ionization energy of structure **2**. As reported in Table 1 the BLYP ionization energy is lower by 71.2 kcal mol^{-1} compared with the non-complexed ethylene (**1**). Although this value most likely also suffers from the described self-interaction errors of the BLYP functional, it nevertheless favors the localization of charge on the ethylene moiety. These results suggest that the problem of artificially delocalized electron densities decreases for short C–O distances. This point can readily be verified in our case by performing single point energy calculations on the subsystems shown in Figure 5b (i.e., at ionization in run **B**) and 5c (i.e., at closest ethylene–water approach in run **B**) using the standard 6–31+G(d,p) basis set and the BLYP, B3LYP, and BHLYP density functionals as well as the Hartree–Fock method as implemented in Gaussian 94.[28] The cumulative Mulliken charges calculated for the C_2H_4 subunit of the supermolecule in 5b, which bears an overall unit positive charge, is +0.24, +0.36, +0.74, and +0.86 at the BLYP, B3LYP, BHLYP, and HF level of theory, respectively. The same trend is found using CHELPG charges.[31] For the structure depicted in 5c the localization of the charge at the ethylene subunit is more pronounced. The Mulliken charges found here amount to +0.31, +0.51, +0.69, +0.79 given in the same order as above. The differences observed between the structures in 5b and 5c indicate that charge localization at the ethylene moiety occurs at least to some extent as soon as water molecules approach close enough to one of the ethylene carbon atoms in an orientation that is favorable for the addition process.

Despite these technical difficulties, simulations **A** and **B** can still be considered to describe two different, but equally relevant parts of the solution chemistry of alkene radical cations in water. This can be seen by inspecting the "trace" of both simulations as given in Figure 8 in a coordinate system spanned by the C–C and C–O distances. The conformational

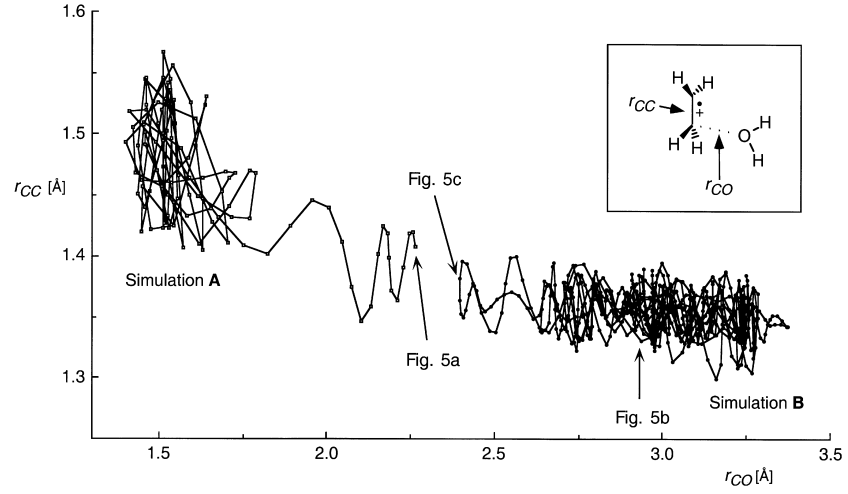

Figure 8. Comparison of simulation **A** (squares) and **B** (circles) in the r_{CC} vs r_{CO} coordinate sytem.

0947-6539/00/0621-4014 $ 17.50+.50/0 *Chem. Eur. J.* **2000**, *6*, No. 21

space explored in simulation **B** is located in the lower right quarter of Figure 8. The trajectory of closest approach carries the system almost, but not quite, to the starting point of simulation **A**, which covers the conformational space in the upper left portion of Figure 8. The transition region for the water addition reaction in aqueous solution will likely be located in the small separating region between simulations **A** and **B** at C–O bond distances around 2.3–2.4 Å.

This finding can be used in order to unify previous experimental and theoretical conclusions as outlined in the introduction. A hydrophobic closed shell molecule such as neutral ethylene acquires a solvent shell characterized through a minimum of solute-solvent and a maximum of solvent–solvent interactions in water (or other protic media). Upon ionization the reorganization of the solvent shell and in particular the creation of a sterically favorable configuration for nucleophilic attack requires time. The associated time scale is set by the *intrinsic* solvent dynamics close to the solute. Thus, the reaction cannot occur instantaneously but is "hindered" due to solvation. However, once a favorable situation for the addition is established due to solvent fluctuations, the reaction occurs readily without further barrier. This latter step of the full reaction is well known from previous theoretical and experimental gas phase studies.

Conclusion

The solvation and subsequent addition and deprotonation reaction of the ethylene radical cation in water was investigated using Car–Parrinello molecular dynamics. Based on two qualitatively different starting configurations, one representing favorable and the other unfavorable initial conditions for an addition to occur, it is found that the reaction occurs readily after a suitable solvent reorganization has taken place. This is in line with both experimental solution phase and theoretical gas phase studies, thus reconciling conflicting results. In contrast to the gas phase situation it is found that the primary addition process is followed by a rapid deprotonation step in aqueous solution via a fast proton transfer to a neighboring water molecule which is "undercoordinated". In fact the lifetime of the initially formed distonic radical cation appears to be less than 100 fs. The processes of addition, bond formation, and subsequent deprotonation are thus tightly coupled in aqueous solution.

Acknowledgement

This work was supported by the Volkswagenstiftung and by a very generous allocation of computer time by the Zuse-Rechenzentrum Berlin. We gratefully acknowledge the help of Dr. J. Hutter with the CPMD code and of Dr. T. Steinke with the infrastructure of the Zuse-Rechenzentrum Berlin.

[1] a) G. Behrens, G. Koltzenburg, D. Schulte-Frohlinde, *Z. Naturfosch. C* **1982**, *37*, 1205; b) G. Koltzenburg, G. Behrens, D. Schulte-Frohlinde, *J. Am. Chem. Soc.* **1982**, *104*, 7311; c) B. Giese, X. Beyrich-Graf, J. Burger, C. Kesselheim, M. Senn, T. Schäfer, *Angew. Chem.* **1993**, *105*, 1850; *Angew. Chem. Int. Ed. Engl.* **1993**, *32*, 1742; d) E. Meggers, A. Dussy, T. Schäfer, B. Giese, *Chem. Eur. J.* **2000**, *6*, 485.

[2] For a review see: M. Schmittel, A. Burghart, *Angew. Chem.* **1997**, *109*, 2658; *Angew. Chem. Int. Ed. Engl.* **1997**, *36*, 2550.

[3] H. Zipse, *J. Am. Chem. Soc.* **1995**, *117*, 11798.

[4] M. Mohr, H. Zipse, D. Marx, M. Parrinello, *J. Phys. Chem. A* **1997**, *101*, 8942.

[5] a) H. J. P. de Lijser, D. R. Arnold, *J. Org. Chem.* **1997**, *62*, 8432; b) H. J. P. de Lijser, D. R. Arnold, *J. Phys. Chem. A* **1998**, *102*, 5592, and references therein.

[6] O. Brede, F. David, S. Steenken, *J. Chem. Soc. Perkin Trans. 2* **1995**, 23.

[7] a) L. Johnston, N. P. Schepp, *J. Am. Chem. Soc.* **1993**, *115*, 6564; b) N. P. Schepp, L. Johnston, *J. Am. Chem. Soc.* **1994**, *116*, 6895; c) N. P. Schepp, L. Johnston, *J. Am. Chem. Soc.* **1996**, *118*, 2872.

[8] A. G. Griesbeck, O. Sadlek, K. Polborn, *Liebigs Ann.* **1996**, 545.

[9] G. Mirafzal, T. Kim, J. Liu, N. L. Bauld, *J. Am. Chem. Soc.* **1992**, *114*, 10968.

[10] F. D. Lewis, M. Kojima, *J. Am. Chem. Soc.* **1988**, *110*, 8664.

[11] R. Car, M. Parrinello, *Phys. Rev. Lett.* **1985**, *55*, 2471.

[12] M. Sprik,J. Hutter, M. Parrinello, *J. Chem. Phys.* **1996**, *105*, 1142.

[13] a) D. Marx, J. Hutter, M. Parrinello, *Chem. Phys. Lett.* **1995**, *241*, 457; b) M. Tuckerman, K. Laasonen, M. Sprik, M. Parrinello, *J. Chem. Phys.* **1995**, *103*, 150.

[14] A. Curioni, M. Sprik, W. Andreoni, H. Schiffer, J. Hutter, M. Parrinello, *J. Am. Chem. Soc.* **1997**, *119*, 7218.

[15] a) D. S. Hartsough, K. M. Merz, Jr. *J. Phys. Chem.* **1995**, *99*, 384; b) W. L. Jorgensen, J. K. Buckner, S. E. Huston, P. J. Rossky, *J. Am. Chem. Soc.* **1987**, *109*, 1891. The solvation of unsymmetrical carbocations has also been studied using a similar approach: P. R. Schreiner, D. L. Severance, W. L. Jorgensen, P. v. R. Schleyer, H. F. Schaefer III, *J. Am. Chem. Soc.* **1995**, *117*, 2661.

[16] BOSS, Version 3.4, W. L. Jorgensen, Yale University, New Haven, CT, **1992**.

[17] CPMD, J. Hutter, P. Ballone, M: Bernasconi, P. Focher, E. Fois. S. Goedecker, M. Parrinello, M. Tuckerman, MPI für Festkörperforschung and IBM Zürich Research Laboratory, **1995–1999**.

[18] a) A. D. Becke, *Phys. Rev. A* **1988**, *38*, 3098; b) C. Lee, W. Yang, R. G. Parr, *Phys. Rev. B* **1988**, *37*, 785.

[19] N. Troullier, J. L. Martins, *Phys. Rev. B* **1991**, *43*, 1993.

[20] D. Marx, M. Sprik, M. Parrinello, *Chem. Phys. Lett.* **1997**, *273*, 360.

[21] The cutoff value of 3.25 Å is determined by the location of the first minimum of g_{00} of BLYP water (see ref. [10]). The same picture is obtained using a larger O–O cutoff distance of 3.3 Å. With a smaller cutoff distance of 3.2 Å, the numbers of nearest water molecules are four for the more reactive and three for the less reactive water molecule, thus leading to the same qualitative finding.

[22] M. Tuckerman, K. Laasonen, M. Sprik, M. Parrinello, *J. Phys. Chem.* **1995**, *99*, 5749.

[23] D. Marx, M. E. Tuckerman, J. Hutter, M. Parrinello, *Nature* **1999**, *397*, 601.

[24] M. Sodupe, J. Bertran, L. Rodriguez-Santiago, E. J. Baerends, *J. Phys. Chem. A* **1999**, *103*, 166.

[25] T. Bally, G. N. Sastry, *J. Phys. Chem. A* **1997**, *101*, 7923.

[26] Y. Zhang, W. Yang, *J. Chem. Phys.* **1998**, *109*, 2604.

[27] J. P. Perdew, A. Zunger, *Phys. Rev. B* **1981**, *23*, 5048.

[28] *Gaussian 94*, Revision E.2, M. J. Frisch, G. W. Trucks, H. B. Schlegel, P. M. W. Gill, B. G. Johnson, M. A. Robb, J. R. Cheeseman, T. Keith, G. A. Petersson, J. A. Montgomery, K. Raghavachari, M. A. Al-Laham, V. G. Zakrzewski, J. V. Ortiz, J. B. Foresman, C. Y. Peng, P. Y. Ayala, W. Chen, M. W. Wong, J. L. Andres, E. S. Replogle, R. Gomperts, R. L. Martin, D. J. Fox, J. S. Binkley, D. J. Defrees, J. Baker, J. P. Stewart, M. Head-Gordon, C. Gonzalez, J. A. Pople, Gaussian, Inc., Pittsburgh PA, **1995**.

[29] S. G. Lias, J. E. Bartmess, J. F. Liebmann, J. L. Holmes, R. D. Levin, W. G. Mallard, "Ion Energetics Data" in *NIST Chemistry WebBook*, *NIST Standard Reference Database Number 69* (Eds.: W. G. Mallard, P. J. Lindstrom), National Institute of Standards and Technology, Gaithersburg, MD, 20899, USA, November **1998** (http://webbook.nist.gov).

[30] A table with energies of all optimized states is contained in the Supporting Information.

[31] C. M. Breneman, K. B. Wiberg, *J. Comput. Chem.* **1990**, *11*, 431.

[32] D. Marx, J. Hutter in *Modern Methods and Algorithms of Quantum Chemistry* (Ed.: J. Grotendorst), Forschungszentrum Jülich (Germany), **2000**.

Received: April 3, 2000 [F2402]